ИНСТИТУТ ЯДЕРНОЙ ФИЗИКИ
им. Г.И. Будкера СО РАН

K. Melnikov, M. Spira, O. Yakovlev

THRESHOLD EFFECTS IN TWO-PHOTON DECAYS OF HIGGS PARTICLES

BudkerINP 94-39

НОВОСИБИРСК

Threshold Effects in Two–Photon Decays

Kirill Melnikov[1], *Michael Spira*[2] *and Oleg Yakovlev*[2,3]

Budker Institute of Nuclear Physics
630090, Novosibirsk 90, Russia

ABSTRACT

The couplings of Higgs particles to two photons are analyzed in the threshold region, where the Higgs mass is about twice the loop–particle mass leading to possible bound state formation. The amplitude of the pseudoscalar decay $A \to \gamma\gamma$ for pseudoscalar masses in the range of $(t\bar{t})$–bound state masses is calculated in leading and next–to–leading order in α_s. It is shown that the real and imaginary parts of the form factor are significantly different from the lowest order perturbative one.

[1] Novosibirsk State University, Novosibirsk–90, Russia
[2] Theory Division, DESY, D–22603 Hamburg, FRG
[3] Budker Institute of Nuclear Physics, Novosibirsk–90, Russia

1 Introduction

The Standard Model [$\mathcal{SM}$] has been tested to a very high precision in recent years. However, the Higgs boson, one of the elementary particles of this model, has not been discovered until now. Higgs boson hunting remains one of the most important problems in contemporary high energy physics. Recently the two–photon decay mode of the Higgs boson attracted much attention by both theorists and experimentalists based on two different reasons:

1. This decay channel provides an opportunity to discover and study the Higgs boson in the lower part of the intermediate mass region at hadron colliders such as the LHC [1].

2. Two–photon production of a heavy Higgs boson via $\gamma\gamma \to H \to ZZ, b\bar{b}, t\bar{t}$ is quite interesting and promising for future high energy $\gamma\gamma$ colliders [2]. Scalar Higgs production via photon fusion exhibits a possibility to distinguish between the Higgs boson of the $\mathcal{SM}$ and the light scalar one of the minimal supersymmetric extension of the Standard Model [$\mathcal{MSSM}$] in the case of the pseudoscalar being very heavy and to measure the Higgs parity [3].

In this paper we consider the coupling of scalar as well as pseudoscalar Higgs bosons to two photons. The existence of pseudoscalar Higgs bosons is predicted by e.g. the $\mathcal{MSSM}$. This model contains three neutral Higgs particles: two $\mathcal{CP}$–even scalars h, H and one $\mathcal{CP}$–odd pseudoscalar A. The $\gamma\gamma$ couplings to these particles are mediated by charged heavy particle loops (W–boson, b– and t–quark) as shown in Fig.1. The top quark and W amplitudes

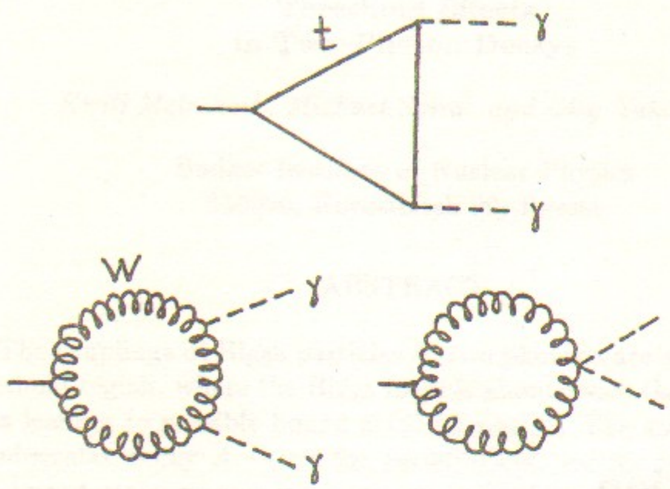

Fig. 1. Generic Feynman diagrams of the $H\gamma\gamma$ and $A\gamma\gamma$ couplings in lowest order: (a) top–loop contributing to the scalar $H\gamma\gamma$ and the pseudoscalar $A\gamma\gamma$ coupling, (b) W–loop contributing to the scalar $H\gamma\gamma$ coupling.

read in lowest order [4]–[6]

$$\begin{aligned} F_t^H &= 2\tau[1+(1-\tau)f(\tau)], \\ F_W^H &= -[3\tau+2-3\tau(\tau-2)f(\tau)], \\ F_t^A &= \tau f(\tau). \end{aligned} \tag{1}$$

The scaling variable is defined as $\tau = 4m_i^2/m_\phi^2$, where m_i denotes the loop–particle mass and m_ϕ the corresponding Higgs mass, and

$$f(\tau) = \begin{cases} \arcsin^2 \dfrac{1}{\sqrt{\tau}} & \tau \geq 1 \\ -\dfrac{1}{4}\left(\log \dfrac{1+\sqrt{1-\tau}}{1-\sqrt{1-\tau}} - i\pi\right)^2 & \tau < 1 \end{cases} \tag{2}$$

The two–loop QCD radiative corrections to the quark amplitudes have been calculated for the scalar Higgs decays [7]–[10] and the pseudoscalar one [11]. Near the $t\bar{t}$–threshold [$\tau \sim 1$] the perturbative result of these corrections to the pseudoscalar top–loop is not valid due to the appearance of a Coulomb singularity originating from possible $(t\bar{t})$–bound state formation in an S–wave. In this mass region the narrow width approximation is not applicable. Due to the quantum numbers of the Higgs particles the intermediate $t\bar{t}$–pairs produced in the scalar Higgs decays $h, H \to t\bar{t} \to \gamma\gamma$ belong to a P–wave amplitude, which is strongly suppressed at threshold leading to negligible effects

of the top decay width and Coulomb interactions of the $t\bar{t}$–pair. Therefore we only consider effects of the W decay width in the scalar decays to photons. The perturbative results for the lowest order amplitudes (1) and the two–loop QCD corrections at threshold are significantly modified due to the following effects:

(i) strong Coulomb interaction of the loop–particles,

(ii) the large width of the t–quark and W–boson.

(iii) mixing of the Higgs bosons with the $t\bar{t}$–bound states [12].

Calculating the form factor of the process $A \to \gamma\gamma$ for $|m_A - 2m_t| \ll m_A$ we have to take into account Coulomb interactions between t and $\bar{t}$. The physical picture is obvious: above threshold, the Coulomb interaction leads to a non–zero probability of $t\bar{t}$ production at $\tau \to 1$, i.e. the imaginary part of F_t^A takes the form [13, 14]

$$\Im m F_t^A = \Im m F_t^{A(LO)} C_{Coul},$$

$$C_{Coul} = \frac{C_F \frac{2\pi\alpha_s}{v}}{1-\exp\left(-C_F \frac{2\pi\alpha_s}{v}\right)}. \tag{3}$$

The parameter $v = \sqrt{1-\tau}$ is the relative velocity of the $t\bar{t}$ pair and $C_F = 4/3$ denotes the usual SU(3)–color factor. The process $A \to t\bar{t} \to \gamma\gamma$ proceeds via an S–wave resulting in an imaginary part of F_t^A in lowest order proportional to v at threshold. After including the perturbative QCD corrections in the narrow width approximation the imaginary part of F_t^A develops a finite step at the $t\bar{t}$–threshold, whereas the real part acquires the corresponding logarithmic singularity for $m_A = 2m_t$. This singular behaviour of the form factor is removed by including the finite decay width of the top quark and Coulomb interactions leading to resonance formation of bound states with quantum numbers $J^{PC} = 0^{-+}$ below threshold. We should note that non–perturbative QCD effects are very important for the bound–state formation, but due to the large width of the top quark they are suppressed in the production of a $t\bar{t}$ system [the relative correction being less than 1%] [16]–[18]. In this paper we take into account the finite width Γ_t of the top quark and Coulomb interaction effects in the threshold region. Qualitatively this analysis leads to the appearance of a finite tail in the imaginary part of F_t^A below threshold and resonance formation of bound states with a finite width $2\Gamma_t$. We present the results for the amplitudes $H \to \gamma\gamma$ and $A \to \gamma\gamma$ in leading and next–to–leading order in α_s.

In order to use those amplitudes for the prediction of the Higgs production cross-section in the vicinity of the loop-particle threshold, one has to include mixing of the Higgs field with $t\bar{t}$–bound states, resulting in important contributions to the decay width in the threshold region. An extensive study of these effects has been performed in Ref.[12], where reader can find all relevant formulas. In the following we will neglect these mixing effects, so that our results correspond to the decays of unmixed Higgs bosons.

2 Coulomb Interactions

The general formula for the amplitudes F_t^A and F_W^H for vanishing decay widths of the top quark and W–boson in the threshold region reads as [see Appendix]:

$$F = A + B\ G(0,0;E) \tag{4}$$

A and B are real constants, determined by a non–relativistic expansion around the threshold of the lowest order form factors (1). $G(0,0;E)$ denotes the S–wave Green's function of the non–relativistic Schrödinger equation with a potential $V(r)$:

$$\left[-\frac{\nabla^2}{m} + V(r) - E\right] G(\vec{r},\vec{r}\,';E) = \delta(\vec{r}-\vec{r}\,')\,. \tag{5}$$

First we consider the pseudoscalar amplitude F_t^A. To determine the Green's function $G_t(0,0;E)$ we have to solve the Schrödinger equation (5) with $m = m_t$ and the Coulomb potential $V(r)$:

$$V(r) = -\frac{4}{3}\frac{\alpha_s}{r}\,. \tag{6}$$

In this section we choose the strong coupling α_s to be constant, whereas effects of a running coupling $\alpha_s(r)$ will be discussed in the next section. Non–perturbative effects of the potential $V(r)$ leading to confinement at large distances are suppressed by the large top decay width and will be neglected in our analysis.

Equation (4) has a clear physical meaning for this amplitude: the process $A \to t\bar{t} \to \gamma\gamma$ is mediated by a quark loop, which quarks contain a large virtuality, or by the formation of $(t\bar{t})$–bound states. These are produced near the origin $r = 0 + \mathcal{O}(m_t^{-1})$, evolve during a time $\tau \sim |E|^{-1}$ and annihilate to two photons at the same point $r = 0 + \mathcal{O}(m_t^{-1})$. So the first term in eq.(4) has a relativistic origin from virtual quark contributions, but the second one

is connected with the non–relativistic dynamics of the $t\bar{t}$ system. Due to bound state formation the form factor $F(E)$ develops poles at $E = E_n$. The constants A, B as well as the position of these poles and their residues can be expressed as expansions in α_s/π:

$$A = \sum_n A_n \left(\frac{\alpha_s}{\pi}\right)^n, \qquad B = \sum_n B_n \left(\frac{\alpha_s}{\pi}\right)^n. \tag{7}$$

Our main goal is the calculation of the short distance coefficients A, B in leading and next–to–leading order in α_s, i.e. the determination of A_0, B_0, A_1 and B_1. In case of a fixed value of α_s these can be obtained from the well–known expression of the Green's function calculated in Ref.[15, 16, 19]:

$$G_t(0,0;E) = -\frac{m_t p}{4\pi} + \frac{m_t p_0}{2\pi}\log\left(\frac{m_t}{p}D\right) + \frac{m_t p_0^2}{2\pi}\sum_{n=1}^{\infty}\frac{1}{n(np-p_0)} \tag{8}$$

with $p_0 = \frac{2}{3}m_t\alpha_s$ and $p = \sqrt{m_t(-E-i\epsilon)}$. D is a real constant depending on the renormalization of the Green's function. The first term in eq.(8) corresponds to the lowest order diagram, the second to the contribution of one coulombic gluon exchange, whereas the third one describes the sum over all bound states with level number n corresponding to diagrams with exchanges of n Coulomb gluons. We note that the uncertaincy from choosing D in (8) is of next–to–leading order in α_s, so that we have to calculate the amplitude F in the two–loop approximation in order to define this constant. These QCD radiative corrections will be discussed in the next section. We choose $D = 1$ in this section for the numerical analysis.

The Green's function of the W–loop contributing to the scalar decays $h, H \to \gamma\gamma$ is given by the first term of eq.(8) being related to the solution of the Schrödinger equation (5) without the potential $V(r)$, because W–bosons do not interact strongly in $\mathcal{O}(\alpha_s)$:

$$G_W(0,0;E) = -\frac{m_W p}{4\pi} \tag{9}$$

with $p = \sqrt{m_W(-E-i\epsilon)}$.

In order to fix the constants A and B we start with the form factors F in one–loop approximation (1). We obtain from a non–relativistic expansion at the threshold:

$$\begin{aligned} A_W^H &= 5 + \frac{3}{4}\pi^2, & B_W^H &= -\frac{12\pi^2}{m_W^2}, \\ A_t^A &= \frac{\pi^2}{4}, & B_t^A &= \frac{4\pi^2}{m_t^2}. \end{aligned} \tag{10}$$

These constants correspond to the lowest order coefficients of the expansions (7) in α_s. As noted above the large value of the t–quark (W–boson) width Γ_t (Γ_W) modifies the properties of the processes $A \to \gamma\gamma$ and $H \to \gamma\gamma$ in the threshold region. In the non–relativistic approximation the denominators of the quark (boson) propogators with momentum $p = (m + \epsilon, \vec{p})$ take the form $2m(\epsilon - \frac{\vec{p}^2}{2m} + i\frac{\Gamma}{2})$ (see [16]). The calculation of the amplitude F is analogous to the case of zero width (see Appendix) leading to the simple replacement

$$E \to E + i\Gamma, \tag{11}$$

in particular $p \to p = \sqrt{m(-E - i\Gamma)} = p_- + ip_+$
with $p_\pm = \sqrt{\frac{m}{2}(\sqrt{E^2 + \Gamma^2} \pm E)}$.

$$\begin{aligned}
\Re e\, G_t(0,0;E+i\Gamma_t) &= -\frac{m_t p_-}{4\pi} + \frac{m_t p_0}{4\pi}\log\left(\frac{p_0^2}{p_+^2+p_-^2}D^2\right) \\
&\quad + \frac{m_t p_0^2}{2\pi}\sum_{n=1}^{\infty}\frac{p_- - p_n}{n^2((p_- - p_n)^2 + p_+^2)}\,, \\
\Im m\, G_t(0,0;E+i\Gamma_t) &= \frac{m_t p_+}{4\pi} + \frac{m_t p_0}{2\pi}\arctan\frac{p_+}{p_-} \\
&\quad + \frac{m_t p_0^2}{2\pi}\sum_{n=1}^{\infty}\frac{p_+}{n^2((p_- - p_n)^2 + p_+^2)}
\end{aligned} \tag{12}$$

$$\text{with} \qquad p_n = \frac{p_0}{n} \qquad \text{and} \qquad p_0 = \frac{2}{3}m_t\alpha_s\,.$$

For our numerical calculation we have used the Standard Model t quark width [20]:

$$\Gamma_t = \frac{G_F m_t^3}{8\pi\sqrt{2}}\left(\frac{2k}{m_t}\right)\left[(1-x^2)^2 + (1+x^2)y^2 - 2y^4\right]\,, \tag{13}$$

where $x = m_b/m_t$, $y = m_W/m_t$ and k is the 3–momentum of the decay products in the t rest frame: $k = \frac{1}{2}\sqrt{[1-(x+y)^2][1-(x-y)^2]}$. Further we choose $m_t = 140$ GeV, $m_b = 5$ GeV, $m_W = 80.14$ GeV, $\alpha_s = 0.15$ and $\Gamma_W = 2.15$ GeV.

The results for $\Re eF_W^H$, $\Im mF_W^H$ and $\Re eF_t^A$, $\Im mF_t^A$ are plotted in Figs.2 and 3 respectively. The effect of the W decay width (Fig.2) to the scalar decays $h, H \to \gamma\gamma$ amounts to about 15% at the W^+W^-–threshold rapidly decreasing apart from the threshold region.

We observe from Fig.3 that $\Im mF_t^A$ contains a peak at the energy of the lowest $(t\bar{t})$–bound state, but $\Re eF_t^A$ shows a maximum on the left–hand side of

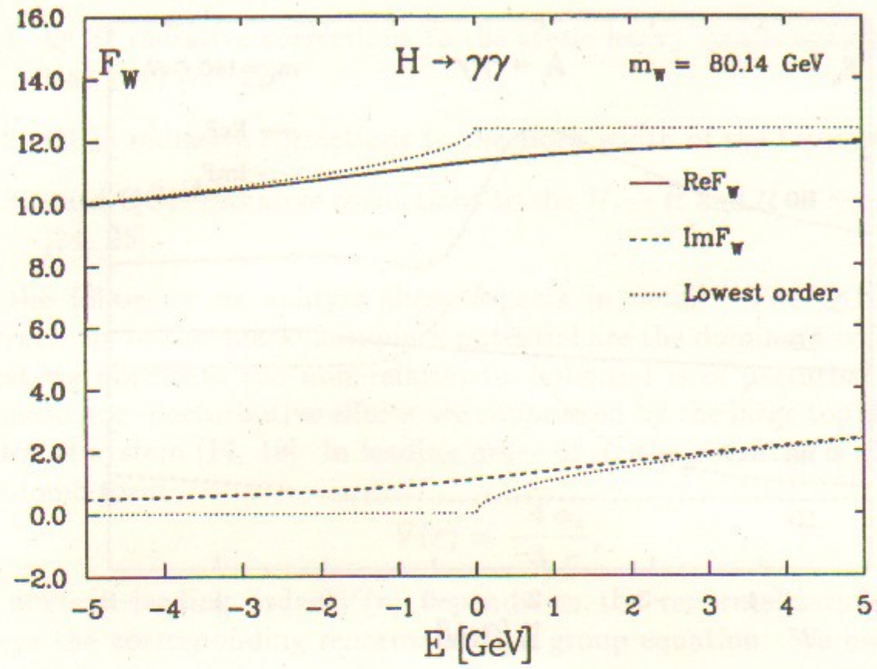

Fig. 2. W–loop form factor F_W^H of the scalar Higgs decays $h, H \to \gamma\gamma$ plotted versus the distance $E = m_H - 2m_W$ to the W^+W^-–threshold. The results including the decay width Γ_W are compared to the lowest order perturbative ones.

this energy level and a minimum on the right–hand side. This behaviour can easily be understood in the narrow–width approximation ($\Gamma_t \ll |E|$) leading to a qualitative picture of the result. Consider F_t^A at $E \to E_n$, where E_n is the bound state energy of level n. The Green's function contains a pole at $E = E_n - i\Gamma_t$. Keeping the leading term of $G(0,0;E)$ only we obtain

$$F_t^A(E) = A_0 + B_0\frac{|\Psi_0(0)|^2}{E_0 - E - i\Gamma_t}, \tag{14}$$

$\Psi_0(0)$ denotes the lowest level wave function of the Coulomb potential at the origin, for arbitrary n given by $|\Psi_n(0)|^2 = k_n^3/\pi$ with $k_n = \frac{2}{3}m_t\alpha_s/(n+1)$. The first term in (14) is a real constant, the imaginary part of the second develops a maximum at $E = E_0$, but the real part vanishes there showing a maximum for $E < E_0$ and a minimum at $E > E_0$.

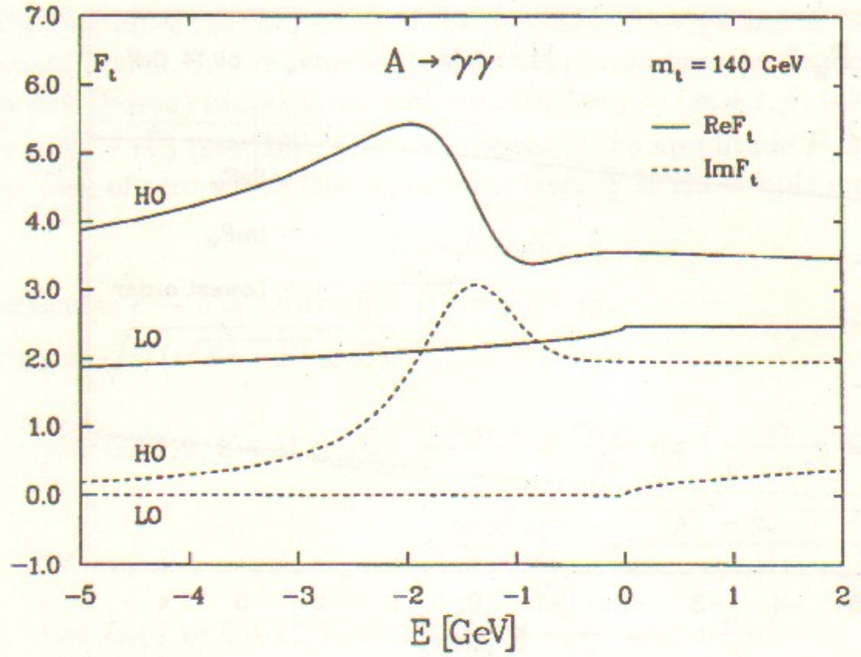

Fig. 3. Top–loop form factor F_t^A of the pseudoscalar Higgs decay $A \to \gamma\gamma$ plotted against the deviation $E = m_A - 2m_t$ from the $t\bar{t}$–threshold for a QCD–potential with constant $\alpha_s = 0.15$. The results including the complete Green's function $G_t(0,0;E+i\Gamma_t)$ (HO) are compared to the lowest order perturbative ones (LO).

3 QCD Corrections

In this section the QCD corrections to the $A\gamma\gamma$ amplitude at the threshold $m_A = 2m_t$ are calculated. First we consider the exact result for the two–loop QCD corrections to the $A\gamma\gamma$ vertex [11]. In order to obtain the radiative corrections to the coefficient A of eq.(4) we must extract the contribution of one Coulomb gluon exchange from the exact two–loop result $[B\frac{m_t p_0}{2\pi}\log(\frac{m_t D}{p})]$, which is already absorbed in the Green's function (8). After this subtraction we obtain

$$\begin{aligned} A &= A_0\left(1+a\frac{\alpha_s}{\pi}\right), \\ a &\approx -4.86 \qquad \text{for } D=1\,. \end{aligned} \tag{15}$$

We should note that the constant a depends on the parameter D, but the total result for the form factor F_t^A does not depend on D. There are three

sources of radiative corrections to the second term in eq.(4):

1. QCD radiative corrections to the static heavy quark–antiquark potential $V(r)$ [21, 22],
2. QCD radiative corrections to the Born width of the top quark [23],
3. hard QCD radiative corrections to the $H \to t\bar{t}$ and $t\bar{t} \to \gamma\gamma$ amplitudes [24, 25].

In the following we analyze these aspects in detail. The QCD radiative corrections to the quark–antiquark potential are the dominant contributions. First we note that the non–relativistic potential is of perturbative nature, because non–perturbative effects are suppressed by the large top decay width in the $t\bar{t}$ system [17, 18]. In leading order of α_s the potential is given by the Coulomb form

$$V(r) = -\frac{4}{3}\frac{\alpha_s}{r}, \tag{16}$$

In next–to–leading order $V(r)$ depends on the renormalization scale and obeys the corresponding renormalization group equation. We use the QCD potential with running coupling α_s:

$$\alpha_s(r) = \frac{4\pi}{b_0\log((\Lambda r)^{-2}) + b_1/b_0\log\log((\Lambda r)^{-2})}\,, \tag{17}$$

where $b_0 = 11 - \frac{2}{3}n_f$, $b_1 = 102 - \frac{38}{3}n_f$ are the first coefficients in the perturbative expansion of the QCD β–function. The QCD scale is given by [18]

$$\begin{aligned} \Lambda &= \Lambda_{\overline{MS}}\exp\left(\frac{C}{2}\right) \approx 2.43\,\Lambda_{\overline{MS}} \quad (n_f = 5) \\ \text{with} \quad C &= \frac{1}{b_0}\left(\frac{31}{3} - \frac{10}{9}n_f\right) + 2\gamma_E \\ \text{and} \quad \Lambda_{\overline{MS}} &\approx \left(\frac{4\pi}{b_0\alpha_s(M_Z)}\right)^{[b_1/(2b_0^2)]} M_Z \exp\left[-\frac{2\pi}{b_0\alpha_s(M_Z)}\right]. \end{aligned} \tag{18}$$

Following **Ref.**[18] we perform a simple regularization of the pole at $\Lambda r \approx 0.785$ by replacing $\Lambda r \to a\tanh(\Lambda r/a)$ with $a = 0.3$. The final form of the QCD–potential can be expressed as

$$V(r) = -\frac{4}{3}\frac{\alpha_s(r)}{r}, \tag{19}$$

The Green's function $G_t(\vec{r},\vec{r}';E)$ was calculated numerically with an accuracy of 10^{-5}, where we checked the results for the real and imaginary parts using a Coulomb potential with constant α_s against the analytical results (12). As a further check we compared our result for $\Im m G_t(0,0;E)$ using a potential with running α_s with the results of [18, 26, 27] and found full agreement. Only the energy dependent part of $\Re e G_t(0,0;E)$ can be determined by our numerical program, whereas the unknown constant not depending on E can be fixed by comparing our numerical result with the analytical expressions (12) at large energy E, because both results must match in $\mathcal{O}(\alpha_s)$. The numerical results for $\Re e F_t^A$ and $\Im m F_t^A$ are plotted in Fig.4 choosing $\alpha_s(m_Z) = 0.12$.

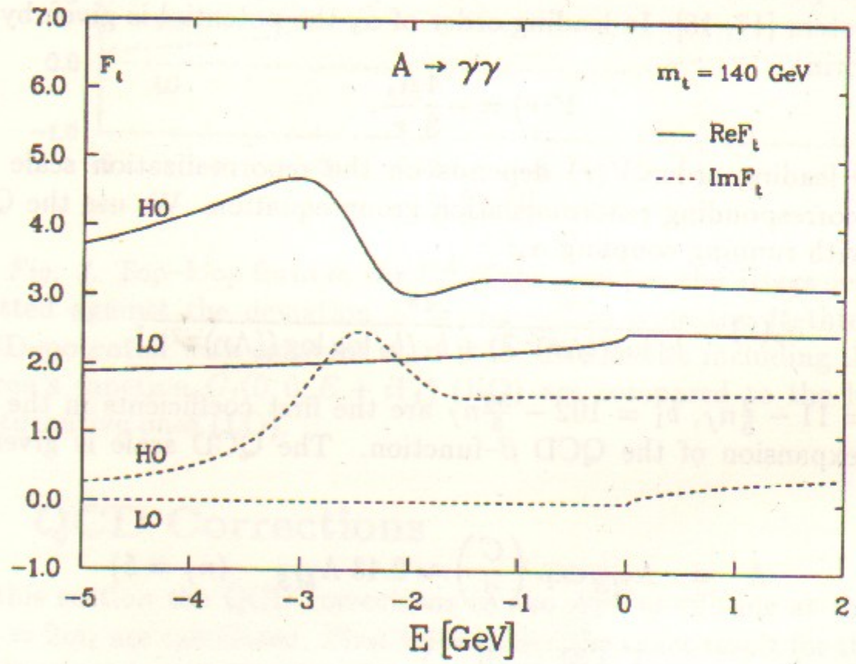

Fig. 4. Same as in Fig.2, but with a QCD–potential using a running α_s normalized to $\alpha_s(M_Z) = 0.12$.

The QCD radiative corrections to the Born width of the top quark were calculated in Ref.[23] and are negligible in our analysis. The third contribution leads to a correction to the constant B in eq.(4)

$$B = B_0 \left(1 + b\frac{\alpha_s}{\pi}\right) , \tag{20}$$

The coefficient b can be obtained analytically from the well–known results of Refs.[24] and [25], because the real corrections to their results belong to a P–wave contribution and therefore vanish at threshold. The hard corrections at threshold to the process $t\bar{t} \to \gamma\gamma$ are given by [24]

$$1 - \frac{\alpha_s(2m_t)}{\pi}\left[\frac{C_F}{2}\left(5 - \frac{\pi^2}{4}\right)\right] \tag{21}$$

and the corresponding ones to $A \to t\bar{t}$ by [25]

$$1 - \frac{\alpha_s(2m_t)}{\pi}\left(3\,\frac{C_F}{2}\right) . \tag{22}$$

The coefficient b is determined by the sum of both contributions:

$$b = -\frac{C_F}{2}\left(8 - \frac{\pi^2}{4}\right) \tag{23}$$

and has been compared to the result of the exact two–loop calculation [11] finding agreement of the two.

4 Conclusions

We have analyzed threshold effects to the photonic decay modes $\phi \to \gamma\gamma$ of the scalar and pseudoscalar Higgs particles in the Standard Model [$\mathcal{SM}$] and the minimal supersymmetric extension [$\mathcal{MSSM}$]. These contributions are generated by the finite decay widths of the top quark and W boson as well as strong Coulomb interactions among $t\bar{t}$ pairs giving rise to bound state formation in the threshold region. [Effects due to the mixing between the Higgs fields and the bound states are important [12], but have not been considered in our analysis.] The top–loop does not contribute significantly in a P–wave to the scalar Higgs decays, resulting in negligible threshold effects. W^+W^- pair production in the scalar case proceeds via an S–wave, so that the inclusion of the W decay width leads to threshold effects of $\mathcal{O}(10\%)$ near the W^+W^-–threshold.

The pseudoscalar decay $A \to \gamma\gamma$ is generated by a virtual $t\bar{t}$ pair in an S–wave. Therefore the inclusion of the top decay width and strong Coulomb interactions leads to large and important contributions to the amplitude. We have presented the full form factor performing a non–ralativistic approximation in the threshold region. The calculated effects are large and cannot be neglected, if the pseudoscalar mass m_A is close to twice the top quark mass

m_t [$|m_A - 2m_t| \ll m_A$]. This analysis completes previous calculations of perturbative QCD corrections to the photonic Higgs decays at the two–loop level [7, 11].

5 Appendix

In this appendix we present the method for our calculation of the amplitudes for $H \to \gamma\gamma$ and $A \to \gamma\gamma$ near the W^+W^- or $t\bar{t}$ threshold. First we consider the process $A \to \gamma\gamma$ near threshold [$m_A = 2m_t + E$ with $|E| \ll m_A$]. $F_t^A(E)$ will be calculated in the Coulomb gauge, which is the most convenient one for non–relativistic problems. The general point of our approach is the division of all Feynman diagrams into two different classes:

(i) Class A contains all diagrams without Coulomb gluon exchanges.

(ii) Class B contains only those which are built–up by at least one Coulomb gluon exchange.

For the calculation of diagrams in class A we may use usual perturbative techniques and expand the result in the small ratio $x = E/m_t$, because it is a regular function of x at the origin $x = 0$. It is well–known that diagrams in class B develop singularities at $x = 0$, which correspond to bound states below threshold and strong interaction effects above threshold, resulting in a logarithmic divergence at $x = 0$. In order to calculate diagrams of Class B we divide the integration over the top momentum p_t into two regions:

(B1) $|p_t| \gg Q$.

(B2) $|p_t| \ll Q$.

Q is an arbitrary scale obeying the condition $p_{non-rel} \ll Q \ll p_{rel}$ with $p_{rel} \sim m_t$ [$p_{non-rel} \sim \sqrt{Em_t}$] determining the characteristic scale of relativistic [non–relativistic] phenomena. Region B1 generates no singularity in E and we can neglect all its non–relativistic effects. In region B2 we may use the non–relativistic approximation for the p_t–integration, in the following analyzed in detail. The form factor F_t^A can be written as [Fig.5]:

$$F_t^A = b \int \frac{d^4p_t}{(2\pi)^4} Tr\left\{S_t(p_t)\Gamma_{At\bar{t}}S_t(p_{\bar{t}})\Gamma_{t\bar{t}\gamma\gamma}\right\}, \qquad (24)$$

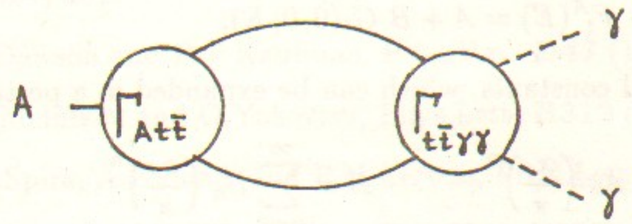

Fig. 5. Diagrammatic representation of the $A\gamma\gamma$ coupling in terms of the vertex operators $\Gamma_{t\bar{t}\gamma\gamma}$ and $\Gamma_{At\bar{t}}$.

where $S_t(p)$ is the fermion propagator and $\Gamma_{At\bar{t}}$ ($\Gamma_{t\bar{t}\gamma\gamma}$) the vertex operator of the corresponding transition. We choose the fermion propagator in its non–relativistic form

$$S_t(p) = \frac{1+\gamma_0}{2}\frac{i}{\varepsilon - \frac{\vec{p}^2}{m_t} + i\frac{\Gamma_t}{2}} \quad \text{with} \quad p = (m_t + \varepsilon, \vec{p}). \qquad (25)$$

We may adopt $\Gamma_{At\bar{t}}$ in the Born approximation, but must take into account all Coulomb gluon exchanges in the $\Gamma_{t\bar{t}\gamma\gamma}$–vertex. One obtains the followig result from this procedure:

$$\Gamma_{t\bar{t}\gamma\gamma}(\vec{p}, E) = \Gamma^0_{t\bar{t}\gamma\gamma}\left\{\frac{\vec{p}^2}{m_t} - E - i\Gamma_t\right\} G_t(\vec{p}; E), \qquad (26)$$

where $\Gamma^0_{t\bar{t}\gamma\gamma}$ is the lowest order coupling of two photons to a $t\bar{t}$ pair at threshold, being independent of $\vec{p}$ and E, and $G_t(\vec{p}; E)$ the Fourier transform of the S–wave Green's function of the non–relativistic Schrödinger equation with the Coulomb potential

$$\begin{aligned}(\hat{H} - E - i\Gamma_t)G_t(\vec{r}, \vec{r}'; E) &= \delta(\vec{r} - \vec{r}') \\ \text{with} \quad \hat{H} &= -\frac{\nabla^2}{m_t} + V(r), \\ V(r) &= -\frac{4}{3}\frac{\alpha_s}{r}, \\ G_t(\vec{p}; E) &= \int d^3\vec{r}\, G_t(\vec{r}, \vec{r}' = 0; E)\, e^{-i\vec{p}\vec{r}}. \end{aligned} \qquad (27)$$

After substituting eqs.(25) and (26) into eq.(24) the p_t^0–integration can be performed explicitly by taking the residue of the pole at $p_t^0 = m_t + \frac{\vec{p}^2}{m_t} - i\frac{\Gamma_t}{2}$. Adding the contributions of class B and those of the class A diagrams we

obtain as the final result

$$F_t^A(E) = A + B\, G_t(0,0;E), \tag{28}$$

where A and B are real constants, which can be expanded in a perturbative series:

$$A = \sum_{n=0}^{\infty} A_n \left(\frac{\alpha_s}{\pi}\right)^n, \qquad B = \sum_{n=0}^{\infty} B_n \left(\frac{\alpha_s}{\pi}\right)^n. \tag{29}$$

The coefficients A_n and B_n can be determined from the comparison with the usual perturbative QCD corrections. The calculation of the amplitude F_W^H is performed in an analogous way without the contribution of the Coulomb potential $V(r)$ by taking into account the W decay width Γ_W only.

Acknowledgements. The authors are grateful to P.M.Zerwas for fruitful discussions and careful reading of the manuscript. K.M. and O.Y. would like to thank P.M.Zerwas for the warm hospitality at DESY, Hamburg.

References

[1] For a recent review see e.g. Z.Kunszt, Zürich report ETH–TH–92–20.

[2] P.M.Zerwas, Proc. VIII Intern. Workshop on Photon–photon collisions (Shoresh, Jerusalem Hills 1988);
B.Gradzkowski and J.F.Gunion, Phys.Lett.**B294** (1992) 361;
J.F.Gunion and H.E.Haber, Phys.Rev. **D48** (1993) 5109;
D.L.Borden, D.A.Bauer and D.O.Caldwell, Phys.Rev. **D48** (1993) 4018.

[3] M.Krämer, J.Kühn, M.L.Stong and P.M.Zerwas, DESY–93–174, December 1993.

[4] J.Ellis, M.K.Gaillard and D.V.Nanopoulos, Nucl.Phys. **B106** (1976) 292.

[5] A.I.Vainstein, M.B.Voloshin, V.I.Zakharov and M.A. Shifman, Yad. Fiz. **30** (1979) 1368, Sov. J. Nucl. Phys. **30** (1979) 711.

[6] J.F.Gunion, G.Gamberini and S.F.Novaes, Phys.Rev. **D38** (1988) 3481.

[7] H.Zheng and D.Wu, Phys.Rev. **D42** (1990) 3760.

[8] A.Djouadi, M.Spira, J.J.van der Bij and P.M.Zerwas, Phys.Lett. **B257** (1991) 187.

[9] S.Dawson and R.P.Kaufman, Phys.Rev. **D47** (1993) 1264.

[10] K.Melnikov and O.Yakovlev, Phys.Lett. **B312** (1993) 179.

[11] M.Spira, A.Djouadi and P.M.Zerwas, Phys.Lett. **B311** (1993) 255.

[12] M.Drees and K.Hikasa, Phys.Rev. **D41** (1990) 1547.

[13] A.Sommerfeld, *Atombau und Spektrallinien* (Vieweg, Braunschweig, 1939).

[14] A.D.Sakharov, Zh.Eksp.Teor.Fiz. **18** (1948) 631.

[15] M.B.Voloshin, Sov.J.Nucl.Phys. **36** (1982) 143.

[16] V.S.Fadin and V.A.Khoze, JETP Lett. **46** (1987) 525, Sov. J. Nucl. Phys. **48** (1988) 309.

[17] V.S.Fadin and O.I.Yakovlev, Sov.J.Nucl.Phys. **53** (1991) 1053.

[18] M.Strassler and M.Peskin, Phys.Rev. **D43** (1991) 1500.

[19] J.Meixner, Math.Z. **36** (1933) 677.

[20] K.Fujikawa, Prog.Theor.Phys. **61** (1979) 1186;
I.I.Bigi, Y.Dokshitzer, V.A.Khoze, J.Kühn and P.M.Zerwas, Phys. Lett. **B181** (1986) 157.

[21] W.Fischler, Nucl.Phys. **B129** (1977) 157.

[22] A. Billoire, Phys.Lett. **B92** (1980) 343.

[23] M.Jeżabek and J.Kühn, Nucl.Phys. **B314** (1989) 1.

[24] L.M.Brown and R.P.Feynman, Phys.Rev. **85** (1952) 231;
I.Harris and L.M.Brown, Phys.Rev. **105** (1957) 1656.

[25] M.Drees and K.Hikasa, Phys.Lett. **B240** (1990) 455.

[26] M.Jeżabek, J.Kühn and T.Teubner, Z.Phys. **C56** (1992) 653;
M.Jeżabek and T.Teubner, Z.Phys. **C59** (1993) 669.

[27] Y.Sumino, K.Fujii, K.Hagiwara, H.Murayama and C.K.Ng, Phys. Rev. **D47** (1992) 56.